FUNG INSTITUTE
for ENGINEERING LEADERSHIP
UC BERKELEY COLLEGE OF ENGINEERING

Model-Based Control System for Packing a 6-Bar Tensegrity Structure

Justino J Calangi

College of Engineering
University of California, Berkeley

Fung Technical Report No. 2014.05.02
http://www.funginstitute.berkeley.edu/sites/default/files/ControlSystem.pdf

May 2, 2014

The Coleman Fung Institute for Engineering Leadership, launched in January 2010, prepares engineers and scientists – from students to seasoned professionals – with the multidisciplinary skills to lead enterprises of all scales, in industry, government and the nonprofit sector.

Headquartered in UC Berkeley's College of Engineering , the Fung Institute combines leadership coursework in technology innovation and management with intensive study in an area of industry specialization. This integrated knowledge cultivates leaders who can make insightful decisions with the confidence that comes from a synthesized understanding of technological, marketplace and operational implications.

130 Blum Hall #5580 Berkeley, CA 94720-5580 | (510) 664-4337 | www.funginstitute.berkeley.edu

Abstract: Robotics has revolutionized the manufacturing industry by replacing human labor with machines; but in certain fields such as medical or extreme environments, the rigidity of traditional robots fail to function as desired. The National Aeronautics and Space Administration (NASA) Ames Research Center is putting effort in developing a new Entry-Descent-Landing (EDL) robotic concept based on a 6-bar 24-cable tensegrity structure. For ease of deployment, the robotic structure is to be packed into a tight space and the operating conditions for efficiently packing a tensegrity robot is investigated in this paper. This paper shows that model-based controllers (Proportional-Derivative (PD) Control or Linear-Quadratic (LQ) Control) together with feedback linearization is capable of manipulating the robot into a packed configuration. Two packing configurations (triangular and hexagonal) are proposed for packing depending on the actuation ability of the robot.

Model-Based Control System for Packing a 6-Bar Tensegrity Structure

University of California, Berkeley
Fung Institute for Engineering Leadership
Master of Engineering
Mechanical Engineering
May 2014

Justino J Calangi
Project Advisor: Prof. Alice M Agogino
Concentration Advisor: Prof. Masayoshi Tomizuka

Abstract

Robotics has revolutionized the manufacturing industry by replacing human labor with machines; but in certain fields such as medical or extreme environments, the rigidity of traditional robots fail to function as desired. The National Aeronautics and Space Administration (NASA) Ames Research Center is putting effort in developing a new Entry-Descent-Landing (EDL) robotic concept based on a 6-bar 24-cable tensegrity structure. For ease of deployment, the robotic structure is to be packed into a tight space and the operating conditions for efficiently packing a tensegrity robot is investigated in this paper. This paper shows that model-based controllers (Proportional-Derivative (PD) Control or Linear-Quadratic (LQ) Control) together with feedback linearization is capable of manipulating the robot into a packed configuration. Two packing configurations (triangular and hexagonal) are proposed for packing depending on the actuation ability of the robot.

Contents

List of Figures

List of Symbols

x	x-coordinate to center of mass of rod
y	y-coordinate to center of mass of rod
z	z-coordinate to center of mass of rod
θ	Azimuthal angle of rod
ϕ	Polar angle of rod
$\mathbf{q}$	Minimal coordinate with $(x,y,z,\theta,\phi)^T$
L	Length of rod
k	Stiffness of cables
J	Second moment of inertia of rod
$\dot{\theta}$	Rate of change of azimuthal angle
$\dot{\phi}$	Rate of change of polar angle
u	Scalar control input of the system - tensional force of each cable
C	Connectivity matrix of tensegrity
$\mathbf{B}$	State space representation control B matrix
$\mathbf{s}$	Vector between both nodes of a cable
$\mathbf{X}$	States of the tensegrity structure
$\mathbf{U}$	Vector of control inputs to the system
$\mathbf{P}$	Controllability matrix of the system
$\mathbf{V}$	Synthetic input for feedback linearization
$\mathbf{Q}$	Cost matrix for LQR states
$\mathbf{R}$	Cost matrix for LQR inputs

1 Introduction

The introduction of robotics into the manufacturing industry has revolutionized how things are made today. Moreover, the consistency and efficiency of robotic processes far exceeds anything humanly capable. But the field of robotics has not reached its full potential in surroundings with uncertain operating conditions. An example of this would be earthquake or fire rescue missions, where firefighters still risk their lives entering the scene to rescue victims. This begs the question of why the current technology is incapable of solving this problem.

A fundamental principle behind traditional robotic inventions is the rigidity nature of it. Robots are made of rigid bars connected with hinges, bolts, or other hardware. To make matters worse, locomotion of these robots are painfully limited to wheels, belt drives, or other similar mechanisms. The result of this is rovers that look like miniature tanks. In order to find a solution to this rigidity problem, the fundamental structure of a robot had to be investigated, and this paper will look into a tensegrity robot.

This capstone project is in collaboration with The National Aeronautics and Space Administration (NASA) Ames Research Center as part of the Super Ball Bot project [10]. The Super Ball Bot is a robotic structure based on tensegrity structures (discussed below), and this paper focuses on the developement of a model-based controller for packing the Super Ball Bot.

1.1 Tensegrity History

Tensegrity is an acronym for "Tensional Integrity." It was first coined by Richard B. Fuller, who experimented with the structural concept of rigid bodies in compression stabilized by a network of strings in tension as early as in 1927 [14]. This structure, as implied by the name, retains its integrity only through tensile members, most likely cables or strings; whereas compression members (herein called bars) are used to hold the cables in place. Figure 1 shows some illustrations of the structures included in Fuller's tensegrity patent in 1962 [5].

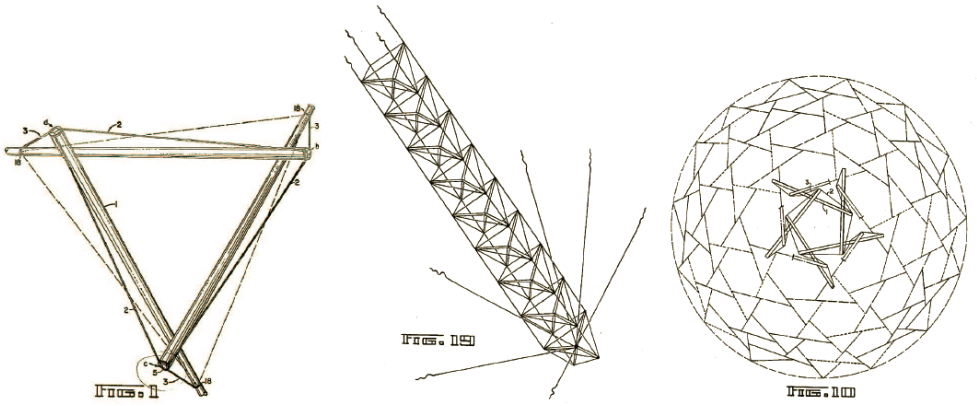

(a) Three strut octahedral tensegrity (b) Tensegrity mast (c) Geodesic dome

Figure 1: Tensegrity illustrations from R B Fuller's 1962 patent[5]

1.2 Tensegrity Structures

Several simple tensegrity structures are illustrated by Snelson's patent in 1965 as shown in Figure 2 [18]. This type of structure is beneficial because it is inherently compliant. If you imagine the cables made up of stretchable materials, like rubber bands, it is apparent that the structure is deformable under different load conditions. In other words, by adjusting the lengths of the cables, we can manipulating this structure such that the shape changes and it can fit into smaller crevices that previous rovers were incapable of reaching. And from this, tensegrity robots are born.

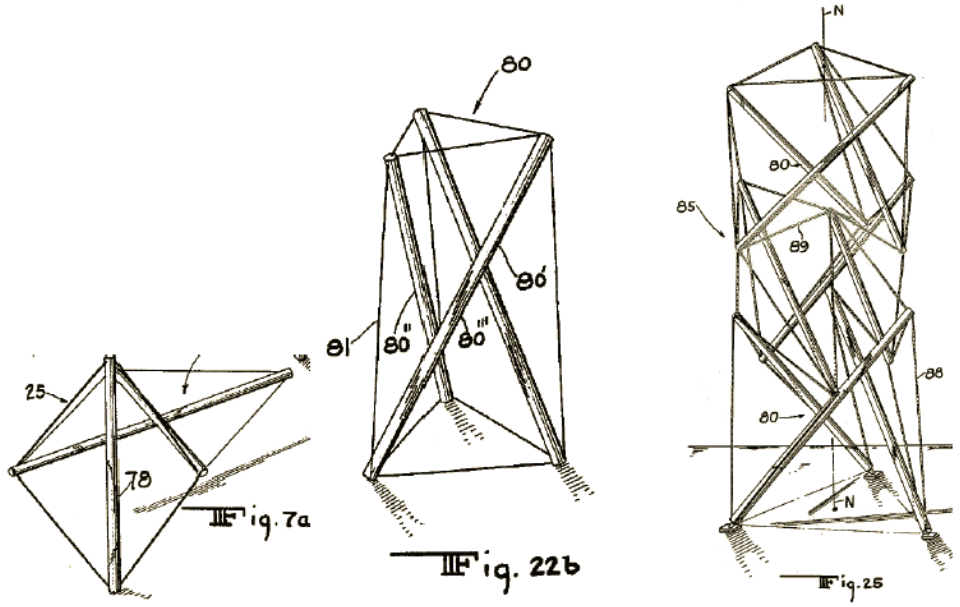

(a) Three strut interconnection (b) Three legged structure (c) Column of three legged structures

Figure 2: Tensegrity illustrations from Snelson's 1965 patent[18]

The tensegrity structure investigated in this paper is a simple **6-bar, 24-cable icosahedron tensegrity structure** (See Section 2 - Mathematical Model for more details). This was chosen because it is the simplest ball-like tensegrity structure, which is beneficial for rolling locomotion.

1.3 Controlling a Tensegrity Robot

Research of controlling tensegrity structures and utilizing them in robotics was first started in the 1990's by Robert E. Skelton and his research group at Purdue University [15,16,17]. His works explored the possibilities of actuating the tensegrity by changing the length of the cables, bars alone, or a combination of both. Moreover, together with Aldrich et al, they studied tensegrity structures in the context of robotics. They presented a feedback linearizarion approach to deployment control of planar tensegrity structures along a predefined path [1, 2]. Anders S Wroldsen, together with Robert E. Skelton and Mauricio C. de Oliveira, also investigated the dynamics and formulation of non-minimal description of the system [21].

Recently, with the goal of exploring Titan in mind, NASA Ames Research Center is currently developing the tensegrity Super Ball Bot[10,11]. To achieve a fast and dynamic tensegrity robot, they developed a simulation environment to using the Bullet Physics Engine. A screenshot of the simulation is shown in Figure 3 [10]. Using this simulation as a platform, Despraz, Iscen and others at Ames have developed an evolutionary control approach through Central Pattern Generation (CPG) algorithms [4,7].

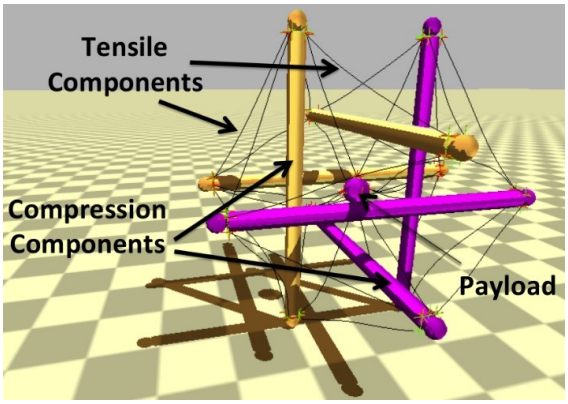

Figure 3: Bullet simulation environment for NASA tensegrity superball[10]

1.4 Packing of a Tensegrity Robot

Aside from locomotion features of the tensegrity structure, in order to efficiently deploy them on missions, packing of the structures are equally important. For this purpose, this paper investigates the control strategy in order to efficiently pack the tensegrity robot for deployment.

An animation from NASA Ames shown in Figure 4 shows the expected packing sequence for the robot[10]. This sequence is taken as a reference in the design, but we will look further into control algorithm development and suggest a more feasible method of packing. While CPG is important for locomotion due to the unknown terrains, packing is proposed to be done with a traditional model-based controller (Proportional-Derivative (PD) control with Feedback Linearization) here.

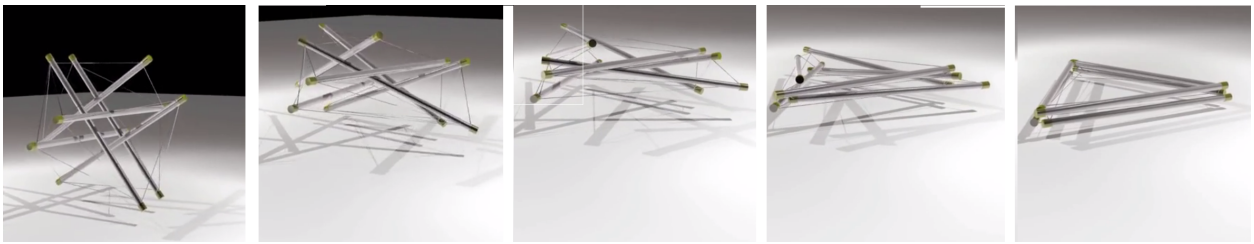

Figure 4: Animation (from left to right) of packing a 6-bar tensegrity robot[10]

2 Dynamics & Mathematical Model

The dynamics of general tensegrity structures are extensively researched and presented in multiple works such as those by Skelton, de Oliveira, Sultan, and Wroldsen et al.[15,19,12, 21]. For the purpose of this paper, we will adopt that of Wroldsen's PhD thesis[21]. His results are presented below and applied to suit the 6-bar tensegrity structure we have. For the complete derivation, please refer to the indicated paper.

2.1 Assumptions

In order to simplify the dynamics for reasonable computation, several basic assumptions are made and presented below:

2.1.1 Rods

- are rigid and inextensible. Hence the length of the rods always remains constant L ;
- are thin cylindrical elements. Hence the rotational motion about its own axis is neglectable.

2.1.2 Cables

- are massless;
- are linear with a stiffness constant of k .

2.1.3 Tensegrity Structure

- is a tensegrity where no rods touch each other;
- is actuated by all cables and no rods.

2.2 Single Rod Dynamics

To describe the tensegrity structure, we first look into the dynamics of a single rod. To generate the ordinary differential equations (ODEs) for the ith rod, we first define the minimal coordinates:

$$\mathbf{q}_i = \begin{bmatrix} x \\ y \\ z \\ \theta \\ \phi \end{bmatrix}_i \tag{1}$$

where $\mathbf{q}_i$ is the minimal coordinate vector that represents the ith rod; x , y , and z are the (x,y,z) coordinates that describe the center of mass of the rod; θ and ϕ are the polar angles to describe the orientation of the rod (see Figure 5).

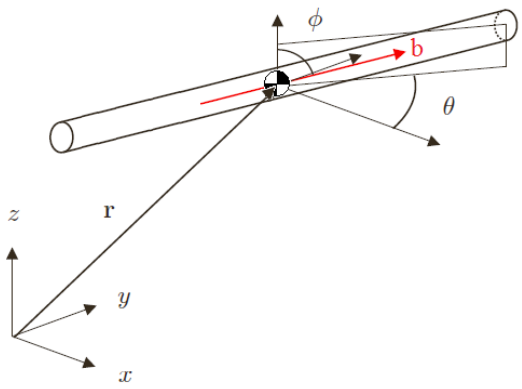

Figure 5: System coordinates to describe a rod

Additionally, the unitary direction vector can be represented by:

$$\mathbf{b}_i = \begin{bmatrix} cos\theta sin\phi \\ sin\theta sin\phi \\ cos\phi \end{bmatrix}_i \tag{2}$$

By ensuring that the position vector is pointing to the center of mass of the rod, the equations of motions of the ith rod with respect to the coordinates $\mathbf{q}$ derived in Wroldsen's paper[21] simplifies to:

$$\mathbf{M}_i(\mathbf{q}_i)\ddot{\mathbf{q}}_i = \mathbf{H}_i(\mathbf{q}_i)(\mathbf{g}_i(\mathbf{q}_i, \dot{\mathbf{q}}_i) + \mathbf{t}_{\mathbf{q}_i}) \tag{3}$$

$$\mathbf{M}_i(\mathbf{q}_i) = \begin{bmatrix} m & 0 & 0 & 0 & 0 \\ 0 & m & 0 & 0 & 0 \\ 0 & 0 & m & 0 & 0 \\ 0 & 0 & 0 & 1 & 0 \\ 0 & 0 & 0 & 0 & 1 \end{bmatrix}_i \in \mathbb{R}^{5\times5} \tag{4}$$

$$\mathbf{H}_i(\mathbf{q}_i) = \begin{bmatrix} 1 & 0 & 0 & 0 & 0 \\ 0 & 1 & 0 & 0 & 0 \\ 0 & 0 & 1 & 0 & 0 \\ 0 & 0 & 0 & \frac{1}{Jsin^2\phi} & 0 \\ 0 & 0 & 0 & 0 & \frac{1}{J} \end{bmatrix}_i \in \mathbb{R}^{5\times5} \tag{5}$$

$$\mathbf{g}_i(\mathbf{q}_i, \dot{\mathbf{q}}_i) = \begin{bmatrix} 0 \\ 0 \\ 0 \\ 2J\dot{\phi}\dot{\theta}\sin\phi\cos\phi \\ J\dot{\theta}^2\sin\phi\cos\phi \end{bmatrix}_i \in \mathbb{R}^5 \tag{6}$$

$\mathbf{t}_{\mathbf{q}}$ represents the generalized forces acting on the rod in terms of the coordinate $\mathbf{q}$. These generalized forces in the unconstrained tensegrity structure are the forces from the cables.

2.3 Cable Forces

The cable forces will also follow the convention presented in Wroldsen's paper[21], first defining $\mathbf{s}_i$ as the vector between the two nodes of the i^{th} string and the scalar control input is defined as each individual cable force:

$$u_i = k(||\mathbf{s}_i|| - l_0) \tag{7}$$

where k is the spring constant of the cable, l_0 is the controllable rest length of the cable. Notice that since the scalar control input u_i is the tensional force of each cable, which indicates that it must be strictly greater or equal to zero. Hence the constraint:

$$u_i \geq 0 \tag{8}$$

2.4 Full Tensegrity Model

For the Super Ball Bot project, the tensegrity structure is a 6-bar icosahedron. For simpler notation, the nodes are assigned as follows:

bar	1	2	3	4	5	6
nodes	$0, 1$	$2, 3$	$4, 5$	$6, 7$	$8, 9$	$10, 11$

Therefore, to have the icosahedron configuration, the connectivity matrix is defined by:

$$C \in \mathbb{R}^{24\times 12} \tag{9}$$

as defined in Appendix A. The 24 rows of the connectivity matrix correspond to the 24 cables that hold the tensegrity structure together, whereas the 12 columns correspond to the 12 end nodes of the 6 rods, and each cable is connected to two nodes.

The resulting tensegrity structure is depicted by the illustration in Figure 6 by Burkhardt [3].

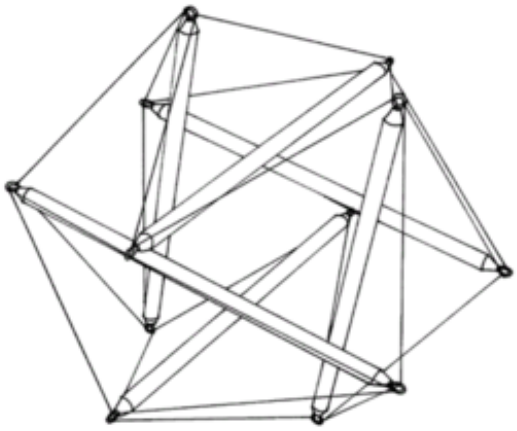

Figure 6: 6-bar, 24-cable icosahedron tensegrity[3]

Since all the rods in the tensegrity structure are strictly independent and only interact through cable forces, the dynamics equations for all six rods can be simply concatenated to form the system coordinate matrix and dynamics equations:

$$\mathbf{M}(\mathbf{q})\ddot{\mathbf{q}} = \mathbf{H}(\mathbf{q})(\mathbf{g}(\mathbf{q},\dot{\mathbf{q}}) + \mathbf{t}_{\mathbf{q}}) \tag{10}$$

where

$$\mathbf{q} = \begin{bmatrix} \mathbf{q}_1 \\ \mathbf{q}_2 \\ \mathbf{q}_3 \\ \mathbf{q}_4 \\ \mathbf{q}_5 \\ \mathbf{q}_6 \end{bmatrix} \in \mathbb{R}^{30} \tag{11}$$

$$\mathbf{M}(\mathbf{q}) = \begin{bmatrix} \mathbf{M}_1(\mathbf{q}) & 0 & 0 & 0 & 0 & 0 \\ 0 & \mathbf{M}_2(\mathbf{q}) & 0 & 0 & 0 & 0 \\ 0 & 0 & \mathbf{M}_3(\mathbf{q}) & 0 & 0 & 0 \\ 0 & 0 & 0 & \mathbf{M}_4(\mathbf{q}) & 0 & 0 \\ 0 & 0 & 0 & 0 & \mathbf{M}_5(\mathbf{q}) & 0 \\ 0 & 0 & 0 & 0 & 0 & \mathbf{M}_6(\mathbf{q}) \end{bmatrix} \in \mathbb{R}^{30\times 30} \tag{12}$$

$$\mathbf{H}(\mathbf{q}) = \begin{bmatrix} \mathbf{H}_1(\mathbf{q}) & 0 & 0 & 0 & 0 & 0 \\ 0 & \mathbf{H}_2(\mathbf{q}) & 0 & 0 & 0 & 0 \\ 0 & 0 & \mathbf{H}_3(\mathbf{q}) & 0 & 0 & 0 \\ 0 & 0 & 0 & \mathbf{H}_4(\mathbf{q}) & 0 & 0 \\ 0 & 0 & 0 & 0 & \mathbf{H}_5(\mathbf{q}) & 0 \\ 0 & 0 & 0 & 0 & 0 & \mathbf{H}_6(\mathbf{q}) \end{bmatrix} \in \mathbb{R}^{30\times 30} \tag{13}$$

$$\mathbf{g}(\mathbf{q},\dot{\mathbf{q}}) = \begin{bmatrix} \mathbf{g}_1(\mathbf{q},\dot{\mathbf{q}}) \\ \mathbf{g}_2(\mathbf{q},\dot{\mathbf{q}}) \\ \mathbf{g}_3(\mathbf{q},\dot{\mathbf{q}}) \\ \mathbf{g}_4(\mathbf{q},\dot{\mathbf{q}}) \\ \mathbf{g}_5(\mathbf{q},\dot{\mathbf{q}}) \\ \mathbf{g}_6(\mathbf{q},\dot{\mathbf{q}}) \end{bmatrix} \in \mathbb{R}^{30} \tag{14}$$

Also, after defining the connectivity matrix, the generalized forces acting on all rods can be written in terms of C and u .

$$\mathbf{t}_{\mathbf{q}} = -\frac{\delta\gamma(\mathbf{q})}{\delta\mathbf{q}}^T \sum_{i=1}^{24} (C_i^T C_i \otimes \mathbf{I}_3)\gamma(\mathbf{q})u_i = \mathbf{B}(\mathbf{q})\mathbf{U} \tag{15}$$

where C_i is the ith row of the connectivity matrix C , and

$$\gamma(\mathbf{q}) = \begin{bmatrix} \mathbf{r}_{n0} \\ \mathbf{r}_{n1} \\ \mathbf{r}_{n2} \\ \mathbf{r}_{n3} \\ \mathbf{r}_{n4} \\ \mathbf{r}_{n5} \\ \mathbf{r}_{n6} \\ \mathbf{r}_{n7} \\ \mathbf{r}_{n8} \\ \mathbf{r}_{n9} \\ \mathbf{r}_{n10} \\ \mathbf{r}_{n11} \end{bmatrix} = \begin{bmatrix} x_1 + \frac{L}{2}\cos\theta_1\sin\phi_1 \\ y_1 + \frac{L}{2}\sin\theta_1\sin\phi_1 \\ z_1 + \frac{L}{2}\cos\phi_1 \\ x_1 - \frac{L}{2}\cos\theta_1\sin\phi_1 \\ y_1 - \frac{L}{2}\sin\theta_1\sin\phi_1 \\ z_1 - \frac{L}{2}\cos\phi_1 \\ \vdots \\ x_6 + \frac{L}{2}\cos\theta_6\sin\phi_6 \\ y_6 + \frac{L}{2}\sin\theta_6\sin\phi_6 \\ z_6 + \frac{L}{2}\cos\phi_6 \\ x_6 - \frac{L}{2}\cos\theta_6\sin\phi_6 \\ y_6 - \frac{L}{2}\sin\theta_6\sin\phi_6 \\ z_6 - \frac{L}{2}\cos\phi_6 \end{bmatrix} \in \mathbb{R}^{36} \tag{16}$$

is the vector of (x ,y ,z)-coordinates of all 12 nodes, and

$$\mathbf{B}(\mathbf{q}) = -\frac{\delta\gamma(\mathbf{q})}{\delta\mathbf{q}}^T [(C_1^T C_1 \otimes \mathbf{I}_3)\gamma(\mathbf{q}) \dots (C_{24}^T C_{24} \otimes \mathbf{I}_3)\gamma(\mathbf{q})] \in \mathbb{R}^{30\times 24} \tag{17}$$

is the matrix that maps the 24 control inputs $\mathbf{U}$ into the 30 states in $\mathbf{q}$. Therefore the model dynamics boil down to

$$\mathbf{M}(\mathbf{q})\ddot{\mathbf{q}} = \mathbf{H}(\mathbf{q})(\mathbf{g}(\mathbf{q}, \dot{\mathbf{q}}) + \mathbf{B}(\mathbf{q})\mathbf{U}) \tag{18}$$

2.5 Dynamics Observations

It is important to note that this dynamics formulation of the tenegrity problem has its own advantages and disadvantages which are also discussed in Wroldsen's paper[21]:
Advantages:

1. This dynamics formulation is fairly common among mechanical systems so various controller designs are available.
2. The chosen coordinate system is such that it is minimal, hence no additional algebraic contraints are necessary when solving the ODE.

Disadvantages:

1. The formulation is such that the ODE inclues many nonlinear components due to the sin and cos manipulations, these nonlinearities are amplified at higher derivatives.
2. There are many singularities within this formulation, one of which is the constraint that ϕ should never be 0 or π (vertical rod). During design it is important to avoid such configurations.

Another simplification made in the formulation of the dynamics is the assumption that there are no constraints on the tensegrity. This assumption is justifiable since we are only investigating packing properties of the structure, where all forces generated in order to pack is purely internal, and that external forces have minimal effects on the procedure.

3 Simulation Tools

3.1 Existing Bullet Simulator

As discussed in Section 1.3, the bullet simulator has helped NASA Ames researchers develop neural evolving control algorithms to roll the tensegrity ball bot. This was possible because Bullet is capable in modelling both high level interaction between the tensegrity structure with the ground, as well as soft cable linkages between individual rigid rods. Moreover, since no user intervention is necessary during the neural learning algorithm, the simulator is programmed such that it is diffcult to obtain intermediate states of the system, which in turn makes traditional control system development (such as state feedback designs) impossible on the simulator.

3.2 MATLAB/Simulink Simulator

With these drawbacks in mind, it was decided that another simulator more suitable for controller development was needed. For this purpose, MATLAB was selected as the platform and the block diagram in Figure 7 below was built using Simulink based on equation (18). As seen in the block diagram, each rod has its own independent dynamics which correspond to the 6 central blocks. The states of each rod is then fed back into a function *StringForces.m* that corresponds to the $\mathbf{B}(\mathbf{q})$ matrix.

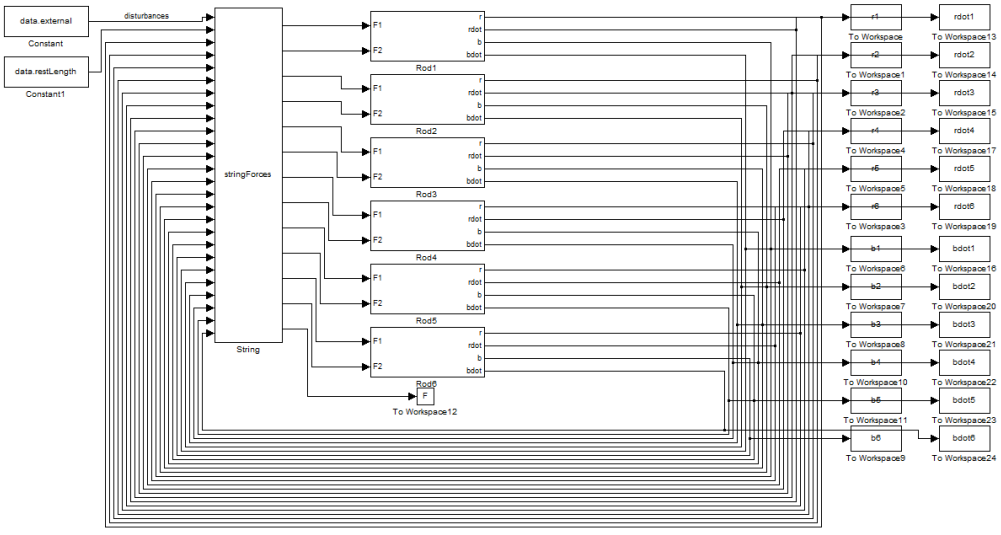

Figure 7: MATLAB/Simulink block diagram of 6-bar tensegrity robot

3.3 MATLAB ode45 solver

In addition to using Simulink for the final simulation and verification, *ode45* in MATLAB was extensively used during the development in order to further explore other types of control strategies such as Model Predictive Control (MPC).

4 Control System Design

4.1 State Space Realization

To begin with the control system design, we first define the state and the system therefore can be represented by the following nonlinear state space representation:

$$\mathbf{X} = \begin{bmatrix} \mathbf{q} \\ \dot{\mathbf{q}} \end{bmatrix} \in \mathbb{R}^{60} \tag{19}$$

$$\dot{\mathbf{X}} = \begin{bmatrix} \dot{\mathbf{q}} \\ \mathbf{M}(\mathbf{q})^{-1}\mathbf{H}(\mathbf{q})\mathbf{g}(\mathbf{q},\dot{\mathbf{q}}) \end{bmatrix} + \begin{bmatrix} \mathbf{0} \\ \mathbf{M}(\mathbf{q})^{-1}\mathbf{H}(\mathbf{q})\mathbf{B}(\mathbf{q}) \end{bmatrix} \mathbf{U} \tag{20}$$

The output equation of the state space representation depends on where sensors are located. For the purpose of this paper, we will assume that all states $\mathbf{X}$ are directly measurable. If this is not the case, the observability conditions need to be investigated:

$$\mathbf{Y} = \mathbf{X} \tag{21}$$

4.2 System Properties

4.2.1 Observations

An outstanding fact when examining this particular tensegrity ball bot structure is that it is *underactuated*. The system itself has 30 degrees of freedom, together with their derivatives make up the state of dimensionalitiy of 60. On the other hand, the configuration of the ball bot only has 24 cables, which in turn manifest as 24 control inputs.

4.2.2 Controllability

For nonlinear systems, controllability can be evaluated using the controllability matrix composed of Lie Brackets [8] in the form of:

$$\mathbf{P} = \begin{bmatrix} g(\mathbf{X}) & [f(\mathbf{X}), g(\mathbf{X})] & [f(\mathbf{X}), [f(\mathbf{X}), g(\mathbf{X})]] & \dots \end{bmatrix} \tag{22}$$

However, due to the complexity of the system, a local controllability approach is done by evaluating:

$$\mathbf{P} = \begin{bmatrix} g(\mathbf{X}_0) & f(\mathbf{X})|_{\mathbf{X}_0} g(\mathbf{X}_0) & f(\mathbf{X})|^2_{\mathbf{X}_0} g(\mathbf{X}_0) & \dots \end{bmatrix} \qquad rank(\mathbf{P}) = 48 \tag{23}$$

As seen from the formulation of the $\mathbf{P}$ matrix, the system is linearized about its initial position (unpacked and standing). Since the linearized system is not full ranked ($48<60$), the system linearized about this initial position is not fully controllable but it may still be accessible, computing the Lie Brackets introduce transcendental nonlinearities and is not done here. We will proceed with the conclusion that there are 12 states that are uncontrollable and identify them further in the paper.

4.3 Feedback Linearization

In order to develop a control system, feedback linearization is used. Feedback linearization aims to linearize the system using the output. In our case as defined by equation (21), output linearization is equivalent to state feedback linearization, which simplifies the formulation of the problem.

We first define a synthetic input such that:

$$\mathbf{V} = \mathbf{M}(\mathbf{q})^{-1}\mathbf{H}(\mathbf{q})\mathbf{g}(\mathbf{q}, \dot{\mathbf{q}}) + \mathbf{M}(\mathbf{q})^{-1}\mathbf{H}(\mathbf{q})\mathbf{B}(\mathbf{q})\mathbf{U} \in \mathbb{R}^{30} \tag{24}$$

The system model from equation (20) then simplifies to:

$$\dot{\mathbf{X}} = \begin{bmatrix} \mathbf{0} & \mathbf{I}_{30} \\ \mathbf{0} & \mathbf{0} \end{bmatrix} \mathbf{X} + \begin{bmatrix} \mathbf{0} \\ \mathbf{I}_{30} \end{bmatrix} \mathbf{V} \tag{25}$$

which is a linear system.

Although this formulation seems simple at first glance, it is important to recall the under-actuated nature of the problem. A major hurdle is that equation (24) presents $\mathbf{V}$ in terms of $\mathbf{U}$. When applying the control, $\mathbf{U}$ has to be computed by:

$$\mathbf{U} = \mathbf{B}(\mathbf{q})^{-1}[\mathbf{H}(\mathbf{q})^{-1}\mathbf{M}(\mathbf{q})\mathbf{V} - \mathbf{g}(\mathbf{q}, \dot{\mathbf{q}})] \tag{26}$$

but $\mathbf{B}(\mathbf{q}) \in \mathbb{R}^{30\times 24}$ is not a square matrix and hence $\mathbf{B}(\mathbf{q})^{-1}$ does not exist.

The use of Moore-Penrose pseudoinverse is proposed here to calculate a "least square" fit to the problem to best approximate the solution. However, this renders the stability of the controller useless since we now have less actuation than degrees of freedom. This feedback linearization technique is used for the development of the Proportional-Derivative (PD) and Linear-Quadratic (LQ) controllers, whereas the development of the Model Predictive Controller (MPC) does not use feedback linearization because the constraints on $\mathbf{U}$ will be hard to implement.

4.4 Controller Design

4.4.1 Proportional-Derivative (PD) Control

Since the system is now linear to V, various control techniques are now available. We will first explore the simple design where:

$$\begin{aligned} \mathbf{V} &= \ddot{\mathbf{q}}_{target} - 2\zeta\omega_n(\dot{\mathbf{q}} - \dot{\mathbf{q}}_{target}) - \omega_n^2(\mathbf{q} - \mathbf{q}_{target}) \\ &= -2\zeta\omega_n\dot{\mathbf{q}} - \omega_n^2(\mathbf{q} - \mathbf{q}_{target}) \end{aligned} \tag{27}$$

where ζ and ω_n are tuning parameters to control the settling time of the tensegrity. Note that $\ddot{\mathbf{q}}_{target} = \dot{\mathbf{q}}_{target} = 0$ and drop out of the equation. An obvious disadvantage of this formulation is that all states are designed to settle at the same rate dependent on ζ and ω_n. An advantage of this formulation is that by picking ζ and ω_n to be positive, the system is guaranteed stability in the linearized form.

4.4.2 Linear-Quadratic (LQ) Control

Linear-Quadratic (LQ) Control is designed to give preference to which states are more important than the others. This optimal control is done by minimizing the quadratic cost function:

$$J = \int_{t_0}^{t_f} (\mathbf{X}^T \mathbf{Q} \mathbf{X} + \mathbf{V}^T \mathbf{R} \mathbf{V}) \tag{28}$$

The controller gains are then obtained by solving the Riccati Equation of the linearized system. As indicated by the feedback linearized system dynamics in equation (25), since (**A,B**) is a controllable pair and (**C,A**) is an observable pair, the LQ formulation is guaranteed robust stability.

4.4.3 Model Predictive Control (MPC)

Model Predictive Control was also attempted during the course of study of the tensegrity ball bot. A major advantage of MPC is that the designer can actively implement constraints onto the control input and states. By implementing a receding horizon control, the optimization algorithm would minimize the cost function similar to that of LQ control over a finite horizon N.

In order to directly implement constraints on the actual control input $\mathbf{U}$, the feedback linearization was not done and the original state space model in equation (20). In order to implement this, Euler's explicit discretization was used:

$$\mathbf{X}(k+1) = \mathbf{X}(k) + dt\dot{\mathbf{X}}(k) \tag{29}$$

$$\begin{bmatrix} \mathbf{q}(k+1) \\ \dot{\mathbf{q}}(k+1) \end{bmatrix} = \begin{bmatrix} \mathbf{q}(k) \\ \dot{\mathbf{q}}(k) \end{bmatrix} + dt \begin{bmatrix} \dot{\mathbf{q}}(k) \\ \mathbf{M}(\mathbf{q}(k))^{-1}\mathbf{H}(\mathbf{q}(k))(\mathbf{g}(\mathbf{q}(k), \dot{\mathbf{q}}(k)) + \mathbf{B}(\mathbf{q}(k))\mathbf{U}) \end{bmatrix} \tag{30}$$

fmincon inside MATLAB was used with the constraints shown in equation (8).

Due to the high degrees of nonlinearities within the system. *fmincon* was unable to find the optimizer $\mathbf{U}$. However, the formulation of the problem in this manner is promising and should be explored further with better numerical optimization algorithms.

5 Simulation Results

5.1 Packing Tensegrity into Triangular Configuration

The initial attempt to fold the tensegrity structure was to follow the animation shown in Figure 4. This was done by contracting the corresponding 12 cables to a target of zero length, and the target state matrix is shown in Appendix B. This resulted in the animation shown in Figure 8.

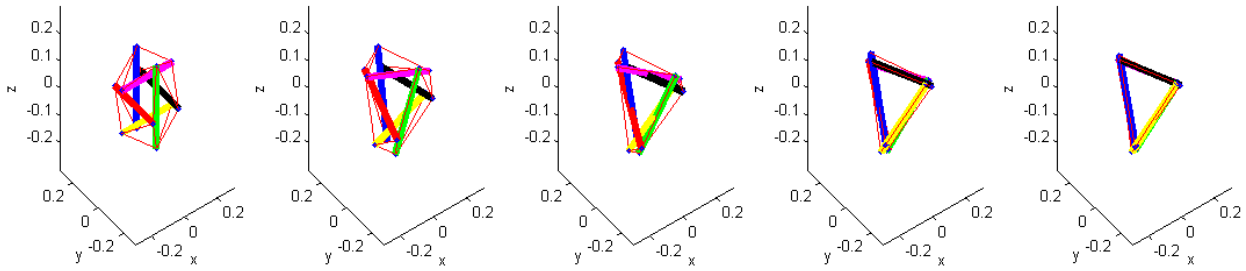

Figure 8: MATLAB simulation of folding a tensegrity structure (left to right)

The corresponding control input in order to pack the structure into the proposed triangular configuration is plotted below in Figure 9. Note that the each cable force corresponds to a unique colored line in the plot. The length of all 24 cables during the process is also plotted in Figure 10.

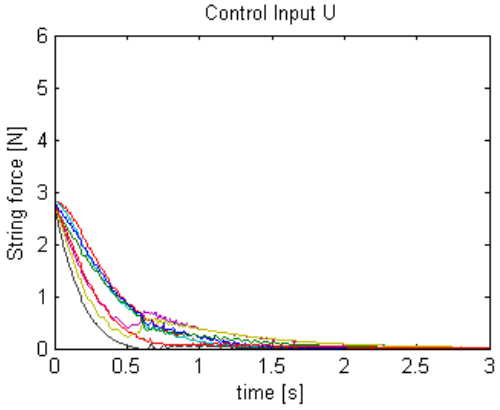

Figure 9: Control input necessary to pack tensegrity into triangle

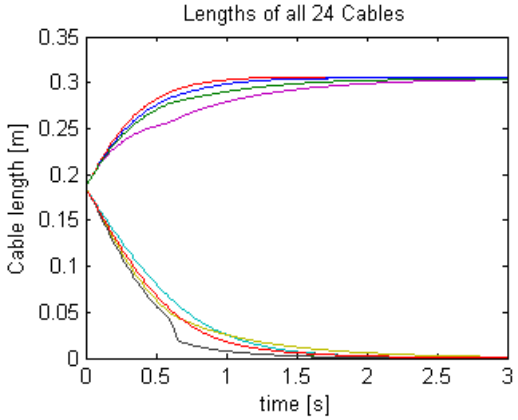

Figure 10: Cable lengths during the packing of tensegrity into triangle

Although this packing scheme is very effective in terms of space, 12 out of the 24 cables need to be fully retracted (lengths go to zero as seen in Figure 10) in order for the nodes to coincide and form the triangle. However, mechanical design of fully retractable cables are not always possible, hence another packing configuration is explored below.

5.2 Packing Tensegrity into Hexagonal Configuration

Instead of having to retract all the cables for packing, another packing configuration in the shape of a hexagon is proposed. This packing shape is the natural collapse configuration of the 6-bar tensegrity structure and a separate simulation of loaded collapse of the structure was done; $\mathbf{q}_{target}$ is shown in Appendix B. Using the hexagonal target configuration, the PD controller was first developed by using the parameters:

$$\zeta = 2, \qquad \omega_n = 10 \tag{31}$$

The reason for these parameters is that the control system must be over damped in order to avoid oscillations. This ensures that the rods remain contactless with each other. ω_n on the other hand controls the settling time of the structure. The resulting simulation is shown below in Figure 11 and the control input necessary is shown in Figure 12.

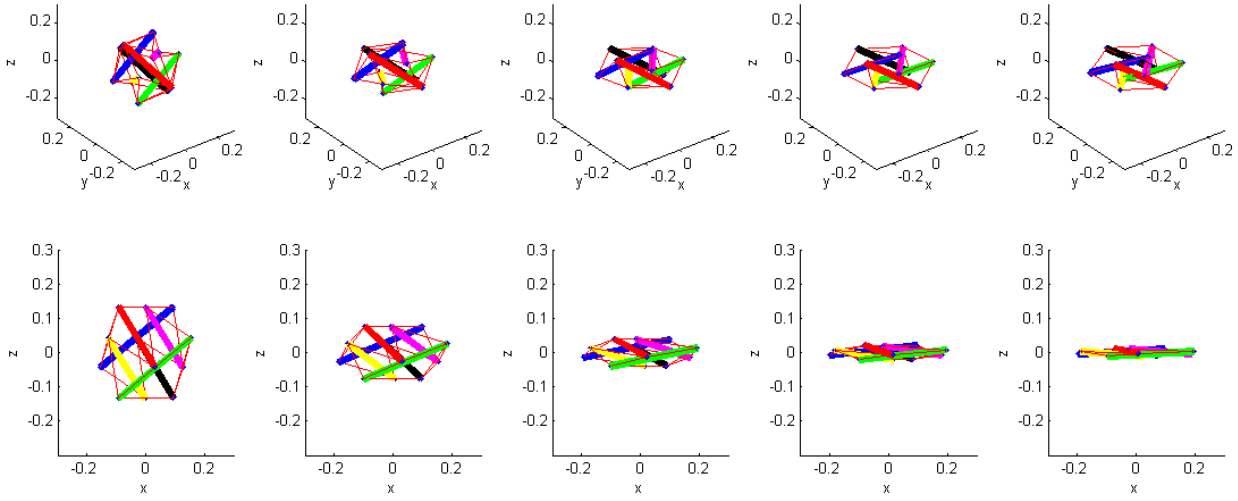

Figure 11: MATLAB simulation of folding a tensegrity structure to hexagonal configuration (left to right). Top: Isometric View, Bottom: Side View

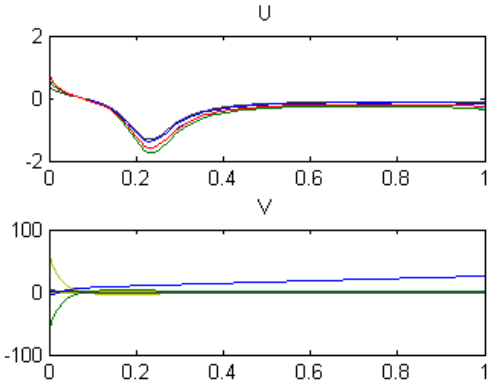

Figure 12: Control input necessary to pack tensegrity into hexagon with PD controller

Notice that the **V** synthetic input is not stable. In fact, when examining the states of each individual rod as shown in Figures 13 and 14, it can be seen that the θ of each rod is unstable. This relates back to previous discussion on controllability of the system. As we mentioned in Section 4.2.2, there are 12 states that are uncontrollable and considered as *internal dynamics*. It is clear from the plot that θ and $\dot{\theta}$ of all rods (a total of 12 states) are unstable. However, aside from those unstable states, the rest all converge to the set targets with no oscillations as designed.

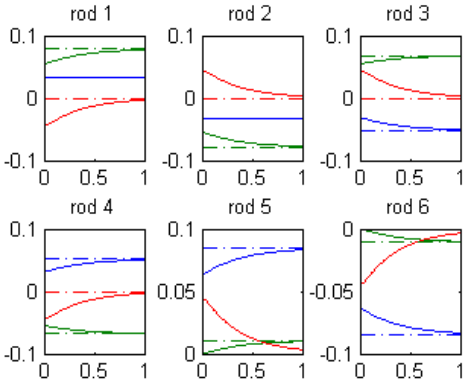

Figure 13: Position coordinates of each rod (x:blue y:green z:red)

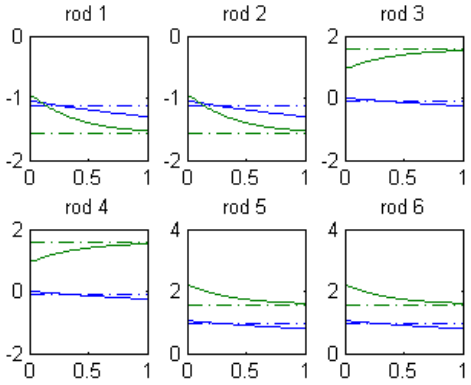

Figure 14: Angular coordinates of each rod (θ:blue ϕ:green)

In addition to the PD controller design, an LQ controller was also proposed with the following **Q** and **R** :

$$\mathbf{Q}_{rod} = \begin{bmatrix} 100 & 0 & 0 & 0 & 0 \\ 0 & 100 & 0 & 0 & 0 \\ 0 & 0 & 100 & 0 & 0 \\ 0 & 0 & 0 & 1 & 0 \\ 0 & 0 & 0 & 0 & 100 \end{bmatrix} \qquad \mathbf{R}_{cable} = 0.001 \tag{32}$$

These values were chosen as an example to emphasize on the states x , y , x , and ϕ , while not being too restrictive on the control input **U** . The results were similar to that of the PD controller and the same phenomenon of unstable θ was observed. This shows that despite a stable controller design after feedback linearization (using LQ or PD), the fact that we are using a "least-squares" approximation with the Moore-Penrose pseudoinverse would destabilize the system and needs to be further investigated.

However, the packing into hexagonal configuration does not require complete retraction of the cable, and hence is a more realistic design for the Tensegrity Super Ball Bot.

6 Conclusions and Future Works

In this paper, the design of a control system for packing the 6-bar 24-cable tensegrity ball bot is investigated. Two major packing configurations (triangular and hexagonal) are proposed and feedback linearization was applied to the minimal dynamics ordinary differential equations.

First and foremost, the minimal coordinates to describe the system has its advantages and disadvantages as discussed in Section 2.5. In order to avoid the nonlinearities, a non-minimal dynamics model is discussed in the works of Skelton [15]. This formulation of the problem also eliminates the singularity condition we see in the ODE formulation where the rod is vertical. Although the formulation has reduced nonlinearities, the tradeoff is that the coordinates are non-minimal and algebraic constraints are necessary. However, this formulation might be more suitable in the implementation of model predictive control algorithms since MPC deals with constraints explicitly while optimizing the cost function.

In addition to the model dynamics, the formulation of the state space realization presented in Section 4.1 assumes that all states are readily available as measurements. In the implementation of the tensegrity robot, it is highly unlikely that all states are measureable. This would introduce the problem of observability of the system and an observer will have to be in place based on the sensors and outputs available. Moreover, sensor noise will have to be taken into account when designing the controller and a Linear-Quadratic Gaussian (LQG) controller might be needed.

Nonetheless, the triangular packing of the tensegrity ball bot is done by fully contracting 12 cables and relaxing the remaining 12 cables. This allows the nodes to overlap with each other and reach the target triangular configuration. An obvious advantage of this packing scheme is the fact that the target configuration is very compact. On the other hand, 12 cables need to be fully retractable in order for this to work, whereas in real prototyping it might be impossible to do so. In order to overcome this drawback, a different packing scheme is investigated.

The hexagonal packing scheme is inspired by the nature collapse of a tensegrity structure under external load. This packing does not require any cable to be fully retractable. In fact, the cables only need to be extendable by 23.1% and retractable by 42.3%. This packing scheme, however, does require full actuation of all 24 cables in order for it to successfully pack. Another drawback of this packing scheme is the control development shown in Section 5.2. Despite the stabilizing controllers developed using the feedback linearization techniques, the fact that the system is underactuated and there are 12 states uncontrollable (See Section 4.2.2) and we are resorting to a least squares estimation destabilizes the system in the θ direction. While this may seem like an issue, it actually is not since the structure is simply rotating on the plane that it has folded. Notice that this is only a problem in this simulation since the tensegrity is currently unconstrained. When external forces such as friction from the ground is acting on the folded structure, it will eliminate the rotation of the structure.

Therefore, packing configuration of the tensegrity structure depends on the mechanical design. If the cables are fully retractable, then packing into a triangle will require nothing more than pulling in 10 cables and relaxing the rest. However, if cables are not fully retractable but fit within the motion bandwidth discussed above, a hexagonal packing configuration is preferred and control algorithms (such as PD, LQ, or MPC) can be developed.

References

[1] J. B. Aldrich. *Control Synthesis for a Class of Light and Agile Robotic Tensegrity Structures.* PhD thesis, University of California at San Diego, Department of Mechanical and Aerospace Engineering, 2004.

[2] J. B. Aldrich and R. E. Skelton. Control/Stucture Optimization Approach for Minimum-Time Reconfiguration of Tensegrity Systems. *In Proceedings of SPIE Smart Structures and Materials: Modeling, Signal Processing and Control*, volume 5049, pages 448-459, San Diego, CA, USA, March 2003.

[3] R. W. Burkhardt, Jr. *A Practical Guide to Tensegrity Design.* 2nd edition. 17 September 2008

[4] J. Despraz. *Super Ball Bot - Structures for Planetary Landing and Exploration.* Master Thesis. Ecole Polytechnique Federale de Lausanne. 16 August, 2013

[5] R. B. Fuller. US Patent 3 063 521 Tensile Integrity Structures. United States Patent Office, 1962.

[6] R. Hollingham. *NASA's 'crazy' robot lab.* 3 February 2013. BBC Future. <http://www.bbc.com/future/story/20130201-nasas-crazy-robot-lab>

[7] A. Iscen, A. Agogino,V. SunSpiral and K. Tumer. *Controlling tensegrity robots through evolution.* In GECCO-2013, Amsterdam, Netherlands, July 2013.

[8] H. K. Khalil. *Nonlinear Systems (Third Edition).* Prentice-Hall Inc., 1996.

[9] R. Motro. *Tensegrity: Structural Systems for the Future.* Kogan Page Science, London, 2003.

[10] NASA. "Final Report: *Super Ball Bot - Structures for Planetary Landing and Exploration* for the NASA Innovative Advanced Concepts (NIAC) Program." July 2013. <http://www.sunspiral.org/vytas/cv/TensegrityPhase1_FinalReport.pdf>

[11] NASA blog. *Presentation on Tensegrity Robots for Planetary Exploration.* 21 March 2013. <https://ti.arc.nasa.gov/blog/irg/?cat=60>

[12] M. C. de Oliveira. Dynamics of Constrained Tensegrity Systems. Technical report, Internal Report, Dynamic Systems Research, Inc., San Diego, CA, USA, August 2005.

[13] M. C. de Oliveira. Dynamics of Systems with Rods. *In Proceedings of the 45th IEEE Conference on Decision and Control*, San Diego, CA, USA, December 2006.

[14] S. Sadao. Fuller on Tensegrity. *International Journal of Space Structures*, 11: 37-42, 1996.

[15] R. E. Skelton. Dynamics and Control of Tensegrity Systems. *In Proceedings of the IUTAM Symposium on Vibration Control of Nonlinear Mechanisms and Structures*, volume 130, Munich, Germany, July 2005.

[16] R. E. Skelton, J. W. Helton, R. Adhikari, J. P. Pinaud, and W. L. Chan. *The Mechanical Systems Design Handbook: Modeling, Measurement, and Control, chapter An Introduction to theMechanics of Tensegrity Structures.* CRC Press, 2001b.

[17] R. E. Skelton, J. W. Helton, R. Adhikari, J. P. Pinaud, and W. L. Chan. An Introduction to the Mechanics of Tensegrity Structures. *In Proceedings of the 40th IEEE Conference on Decision and Control*, Orlando, FL, USA, December 2001a.

[18] K. Snelson. US Patent 3 169 611 Continuous Tension Discontinous Compression Structures. United States Patent Office, 1965.

[19] R. E. Skelton and C. Sultan. Controllable Tensegrity, A New Class of Smart Structures. *In Proceedings of the SPIE 4th Symposium on Smart Structures and Materials*, volume 3039, pages 166-177, 1997.

[20] C. Sultan and R. E. Skelton. Integrated Design of Controllable Tensegrity Structures. *In Proceedings of the ASME International Congress and Exposition*, volume 54, pages 27-37, 1997.

[21] A. S. Wroldsen, M. C. de Oliveira, and R. E. Skelton. A Discussion on Control of Tensegrity systems. *In Proceeding of the 45th IEEE Conference on Decision and Control*, San Diego, December 2006b.

APPENDIX A: Connectivity Matrix

$$C = \begin{bmatrix}
1 & 0 & 0 & 0 & -1 & 0 & 0 & 0 & 0 & 0 & 0 & 0 \\
1 & 0 & 0 & 0 & 0 & -1 & 0 & 0 & 0 & 0 & 0 & 0 \\
1 & 0 & 0 & 0 & 0 & 0 & 0 & 0 & -1 & 0 & 0 & 0 \\
1 & 0 & 0 & 0 & 0 & 0 & 0 & 0 & 0 & 0 & -1 & 0 \\
0 & 1 & 0 & 0 & 0 & 0 & 0 & 0 & -1 & 0 & 0 & 0 \\
0 & 1 & 0 & 0 & 0 & 0 & 0 & 0 & 0 & 0 & -1 & 0 \\
0 & 1 & 0 & 0 & 0 & 0 & -1 & 0 & 0 & 0 & 0 & 0 \\
0 & 1 & 0 & 0 & 0 & 0 & 0 & -1 & 0 & 0 & 0 & 0 \\
0 & 0 & 1 & 0 & -1 & 0 & 0 & 0 & 0 & 0 & 0 & 0 \\
0 & 0 & 1 & 0 & 0 & -1 & 0 & 0 & 0 & 0 & 0 & 0 \\
0 & 0 & 1 & 0 & 0 & 0 & 0 & 0 & 0 & -1 & 0 & 0 \\
0 & 0 & 1 & 0 & 0 & 0 & 0 & 0 & 0 & 0 & 0 & -1 \\
0 & 0 & 0 & 1 & 0 & 0 & -1 & 0 & 0 & 0 & 0 & 0 \\
0 & 0 & 0 & 1 & 0 & 0 & 0 & -1 & 0 & 0 & 0 & 0 \\
0 & 0 & 0 & 1 & 0 & 0 & 0 & 0 & 0 & -1 & 0 & 0 \\
0 & 0 & 0 & 1 & 0 & 0 & 0 & 0 & 0 & 0 & 0 & -1 \\
0 & 0 & 0 & 0 & 1 & 0 & 0 & 0 & -1 & 0 & 0 & 0 \\
0 & 0 & 0 & 0 & 1 & 0 & 0 & 0 & 0 & -1 & 0 & 0 \\
0 & 0 & 0 & 0 & 0 & 1 & 0 & 0 & 0 & 0 & -1 & 0 \\
0 & 0 & 0 & 0 & 0 & 1 & 0 & 0 & 0 & 0 & 0 & -1 \\
0 & 0 & 0 & 0 & 0 & 0 & 1 & 0 & -1 & 0 & 0 & 0 \\
0 & 0 & 0 & 0 & 0 & 0 & 1 & 0 & 0 & -1 & 0 & 0 \\
0 & 0 & 0 & 0 & 0 & 0 & 0 & 1 & 0 & 0 & -1 & 0 \\
0 & 0 & 0 & 0 & 0 & 0 & 0 & 1 & 0 & 0 & 0 & -1
\end{bmatrix} \in \mathbb{R}^{24\times 12} \tag{33}$$

APPENDIX B: Target Configuration

Triangular Packed Configuration:

$$\mathbf{q}_{target} = \begin{bmatrix} 0.0584 \\ 0.0215 \\ 0.0578 \\ -0.8229 \\ -1.3078 \\ -0.0779 \\ 0.0379 \\ -0.0139 \\ 1.2674 \\ 0.7533 \\ -0.0708 \\ 0.0391 \\ -0.0060 \\ 1.2460 \\ 0.7483 \\ 0.0235 \\ -0.0624 \\ -0.0441 \\ -0.0077 \\ 1.0254 \\ 0.0497 \\ 0.0327 \\ 0.0586 \\ -0.7877 \\ 1.7805 \\ 0.0171 \\ -0.0688 \\ -0.0524 \\ -0.0706 \\ 1.0668 \end{bmatrix}$$

Hexagonal Packed Configuration:

$$\mathbf{q}_{target} = \begin{bmatrix} 0.0330 \\ 0.0789 \\ 0 \\ -1.1261 \\ -1.5708 \\ -0.0330 \\ -0.0789 \\ 0 \\ -1.1261 \\ -1.5708 \\ -0.0519 \\ 0.0680 \\ 0 \\ -0.0790 \\ 1.5708 \\ 0.0519 \\ -0.0680 \\ 0 \\ -0.0790 \\ 1.5708 \\ 0.0848 \\ 0.0109 \\ 0 \\ 0.9682 \\ 1.5708 \\ -0.0848 \\ -0.0109 \\ 0 \\ 0.9682 \\ 1.5708 \end{bmatrix}$$